

UC Santa Barbara

UC Santa Barbara Previously Published Works

Title

Improved Elastic Recovery from ABC Triblock Terpolymers.

Permalink

<https://escholarship.org/uc/item/1101b7gn>

Journal

ACS Polymers Au, 3(5)

Authors

Albanese, Kaitlin
Blankenship, Jacob
Quah, Timothy
[et al.](#)

Publication Date

2023-10-11

DOI

10.1021/acspolymersau.3c00012

Peer reviewed

Improved Elastic Recovery from ABC Triblock Terpolymers

Kaitlin R. Albanese, Jacob R. Blankenship, Timothy Quah, Amy Zhang, Kris T. Delaney, Glenn H. Fredrickson, Christopher M. Bates,* and Craig J. Hawker*

Cite This: *ACS Polym. Au* 2023, 3, 376–382

Read Online

ACCESS |

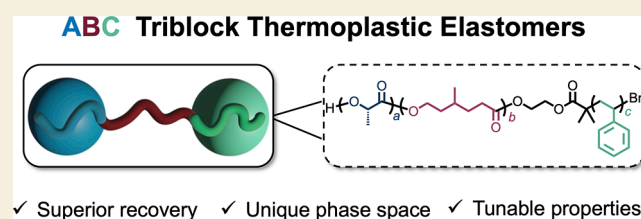
Metrics & More

Article Recommendations

Supporting Information

ABSTRACT: The promise of ABC triblock terpolymers for improving the mechanical properties of thermoplastic elastomers is demonstrated by comparison with symmetric ABA/CBC analogs having similar molecular weights and volume fraction of B and A/C domains. The ABC architecture enhances elasticity (up to 98% recovery over 10 cycles) in part through essentially full chain bridging between discrete hard domains leading to the minimization of mechanically unproductive loops. In addition, the unique phase space of ABC triblocks also enables the fraction of hard-block domains to be higher ($f_{\text{hard}} \approx 0.4$) while maintaining elasticity, which is traditionally only possible with non-linear architectures or highly asymmetric ABA triblock copolymers. These advantages of ABC triblock terpolymers provide a tunable platform to create materials with practical applications while improving our fundamental understanding of chain conformation and structure–property relationships in block copolymers.

KEYWORDS: ABC triblock, thermoplastic elastomer, self-assembly, block copolymer, elastic recovery



INTRODUCTION

Thermoplastic elastomers (TPEs) derived from self-assembled block copolymers are widely used materials due to their synergistic combination of thermal processability and elasticity. Applications range from sealants and adhesives to bio-implants and flexible electronics.^{1,2} Conventional block-copolymer-based TPEs leverage a linear ABA block sequence, e.g., poly(styrene-*b*-butadiene-*b*-styrene), with glassy A domains within a rubbery B matrix. On a molecular level, these symmetric triblocks can adopt two different configurations of B chains that yield very different mechanical performance: bridging between discrete, hard A domains supports stress and imparts elasticity, while any B chains that loop back into the same A domain are mechanically less productive (Figure 1b) unless they physically entangle with other B chains that bridge or loop to a different A domain.^{3,4} To quantify this effect, dynamic viscoelastic measurements^{4,5} and dielectric relaxation³ have been used to experimentally determine the fraction of bridging to looping chains (ϕ_{bridge}) for linear ABA triblock copolymers. This fraction has been shown to depend on morphology with the theoretical value of ϕ_{bridge} calculated to be 0.40–0.45 for lamella, 0.60–0.65 for cylindrical, and 0.75–0.80 for spherical morphologies.^{3,6,7} Strategies to overcome these limitations and increase the bridging fraction to ~ 1.0 would, therefore, enhance mechanical properties^{3,6–8} such as elastic recovery^{9–11} and improve the performance of thermoplastic elastomers.

Initial theoretical and experimental efforts to increase performance and the bridging fraction involved the design of ABABA pentablock copolymers^{12–14} or the synthesis of compositionally asymmetric linear ABA' triblocks¹³ and

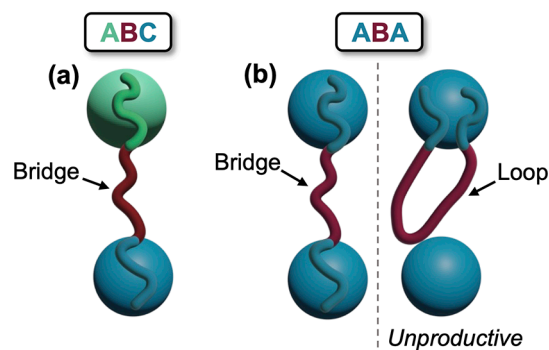


Figure 1. Illustration of (a) the ABC sequence leading to $\sim 100\%$ molecular bridging between two chemically distinct hard domains (A and C). In contrast, (b) both bridge and loop chain configurations arise from an ABA triblock copolymer. Each color represents a different block chemistry.

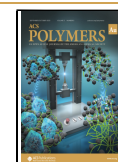
related nonlinear architectures.^{14–16} While these strategies do increase the bridging fraction of B blocks, significant loop formation still occurs. To address this limitation, ABC triblock terpolymers allow for microphase separation between the A and C blocks/domains with minimal to no loops since A

Received: May 17, 2023

Revised: June 15, 2023

Accepted: June 16, 2023

Published: July 18, 2023



chains are not miscible with C domains and C chains are not miscible with A domains (Figure 1a).^{13,17–19} The challenge with ABC triblock terpolymers arise from introducing a third block chemistry that complicates both synthesis and the molecular design—two independent volume fractions (f_A , f_B ; $f_C = 1 - f_B - f_A$) and three Flory–Huggins parameters (χ_{AB} , χ_{AC} , and χ_{BC}) must now be carefully selected. As a result, significantly less work has been devoted to studying ABC TPEs compared to their ABA analogs. In pioneering work, Brinkmann-Rengel and co-workers synthesized poly(styrene-*b*-butadiene-*b*-methylmethacrylate) (S-B-M) via anionic polymerization, but the weak segregation strength ($\chi_{AC}N$) between S and M resulted in mixing of the two hard domains.¹⁹ By incorporating a semicrystalline end block, Abetz and co-workers evaluated the influence of crystallization with poly[styrene-*b*-(ethylene-*stat*-propylene)-*b*-ethylene] (S-EP-E) compared to poly[styrene-*b*-(ethylene-*stat*-propylene)-*b*-styrene] (S-EP-S).¹⁸ At low strains (<300%), S-EP-E showed superior recovery, but at higher strains ($\geq 300\%$) the semicrystalline blocks more easily dislodge from crystalline domains, leading to irrecoverable deformation. Together these papers highlight the potential advantages of ABC triblock terpolymers for enhancing mechanical performance when compared to traditional and widely studied ABA thermoplastic elastomers.

Here, we showcase a novel strategy for the synthesis of high molecular weight ABC triblock terpolymer TPEs via sequential ring-opening polymerizations (ROP) and thermal atom-transfer radical polymerization (ATRP). This use of orthogonal polymerization methods expands the scope of monomers that can be incorporated into block-copolymer-based TPEs as traditional systems utilize anionic polymerization that limits the range of ABC triblock terpolymers that are synthetically accessible.^{18–21} The ABC triblock terpolymers described herein enhance elastic recovery, primarily through full chain bridging with minimal looping due to distinct A and C hard domains. In addition, the unique morphology of ABC triblocks enables the incorporation of larger hard-block volume fractions while maintaining elasticity, a feature that is typically only associated with synthetically challenging non-linear architectures (e.g., asymmetric miktoarm star polymers)²² or asymmetric higher-order block copolymers.⁷ These characteristics of ABC triblock terpolymers highlight a promising strategy for the design of polymeric materials with improved performance while enhancing our fundamental understanding of structure–property relationships.

EXPERIMENTAL SECTION

A key design feature of this study is the ability to prepare ABC and symmetrical ABA or CBC triblocks with similar morphologies and hard-block content that allows for a direct comparison of mechanical performance and, in turn, permits the fundamental role of molecular architecture to be probed. In systematically addressing this opportunity, three different triblocks were synthesized from common synthetic precursors: poly(L-lactide-*b*-4-methylcaprolactone-*b*-styrene) (L-C-S), poly(L-lactide-*b*-4-methylcaprolactone-*b*-L-lactide) (L-C-L), and poly(styrene-*b*-4-methylcaprolactone-*b*-styrene) (S-C-S). These materials were designed to include different glassy or semicrystalline A/C domains while retaining the same rubbery B segments: $T_{g,L} = 60$ °C, $T_{m,L} = 180$ °C, $T_{g,C} = -60$ °C, and $T_{g,S} = 100$ °C.

While Hillmyer and co-workers have reported L-C-L previously,^{23,24} no literature exists for L-C-S and S-C-S. As a result, a modified synthetic strategy to L-C-S triblock terpolymers with varying

volume fractions of the hard blocks (L and S, see Table 1) was developed via sequential ring-opening polymerization (ROP)

Table 1. Molecular Characterization of Different Thermoplastic Elastomers

Sample ^a	f_L^b	f_S^b	$M_{n,\text{total}}^c$	$M_{n,S}^c$	$M_{n,L}^c$	$M_{n,C}^c$	D^d
L-C-S ¹⁸	0.09	0.09	100	9.5	11	80	1.47
L-C-S ²⁰	0.10	0.10	103	10	13	80	1.41
L-C-S ³¹	0.16	0.15	120	18	22	80	1.35
L-C-S ⁴⁰	0.19	0.21	138	28	31	79	1.45
L-C-L ¹⁷	0.17		103		20	83	1.30
L-C-L ²⁰	0.20		108		25	83	1.30
L-C-L ²⁹	0.29		124		41	83	1.36
S-C-S ¹⁷		0.17	95	16		79	1.50
S-C-S ²⁰		0.20	99	20		79	1.50
S-C-S ³⁰		0.30	113	34		79	1.50

^aRefers to block sequence in triblocks with superscripts denoting the total volume percent of hard-block content. ^bCalculated using $\rho_L = 1.25$ g cm⁻³, $\rho_C = 1.037$ g cm⁻³, and $\rho_S = 1.05$ g cm⁻³ at 25 °C.^{24,29}

^cDetermined using end-group analysis via ¹H NMR and reported in kg mol⁻¹. ^dChloroform SEC analysis with PS standards.

followed by atom-transfer radical polymerization (ATRP) (Figure 2). Starting from 2-hydroxyethyl-2-bromoisobutyrate, initial ring-opening polymerization of 4-methylcaprolactone leads to a low T_g central block that can be used to initiate a second ring-opening polymerization of L-lactide to give the L-C diblock copolymer. Significantly, the ATRP chain end is stable under ROP conditions, which allows the diblock copolymer to subsequently initiate thermal ATRP of styrene, leading to the desired L-C-S triblock terpolymers. Size-exclusion chromatography (SEC) indicated successful chain extension of each block as evidenced by a shift to lower retention times while maintaining a symmetric peak shape and low dispersity (Figures S2–S6). The corresponding S-C-S symmetrical triblock analogs were similarly synthesized by initial ROP of 4-methylcaprolactone followed by esterification of the hydroxy chain end with 2-bromo-2-methyl propionyl bromide to give a *bis*-ATRP macroinitiator from which dual end-blocks of polystyrene can be grown (Figures S7–S14). For the L-C-L triblock copolymer, 1,4-*bis*-(hydroxymethyl)-benzene was used as a difunctional initiator for sequential ROP of 4-methylcaprolactone followed by L-lactide with the unique resonances of the phenyl ring allowing for structural characterization and molecular weight determination. For each series of triblocks, a constant midblock molar mass ($M_n \approx 80$ kg mol⁻¹) was targeted to isolate the effects of end-block chemistry and length with all polymers being synthesized in a nitrogen-filled glovebox to ensure high molecular-weight blocks and chain-end fidelity. This allows a library of triblock terpolymers to be synthesized with accurate control over molecular weight and an approximately equal hard-block volume fraction (e.g., $f_{\text{Hard}} = f_L + f_S \approx 0.20$) to facilitate comparisons between L-C-S, L-C-L, and S-C-S derivatives.

To simplify the analysis of phase behavior, Bailey classified triblock copolymers into three groups based on the relative magnitude of pairwise interaction parameters: type-I frustrated ($\chi_{AC} < \chi_{AB} < \chi_{BC}$), type-II frustrated ($\chi_{AB} < \chi_{AC} < \chi_{BC}$), and non-frustrated ($\chi_{AB} < \chi_{BC} < \chi_{AC}$).²⁵ The non-frustrated category is particularly attractive for TPEs since the A and C blocks form two distinct domains rather than more exotic morphologies such as core–shell spheres or cylinders decorated by rings.^{26,27} Here, L-C-S terpolymers were designed as a non-frustrated system with self-assembly into three discrete domains at the molecular weights under study based on previously reported values of $\chi(T)$ for $\chi_{CL} = 0.10$,²⁴ $\chi_{SL} = 0.22$,²⁸ and our estimate of $\chi_{CS} = 0.08$ (all at 23 °C using a reference volume of 118 Å³ and the same ODT predictions). The latter value was experimentally obtained by measuring the order–disorder temperature (T_{ODT}) via rheometry with volumetrically symmetric diblock copolymers that were prepared using a variation of the above strategies (Figure S16a,b and Table S1).

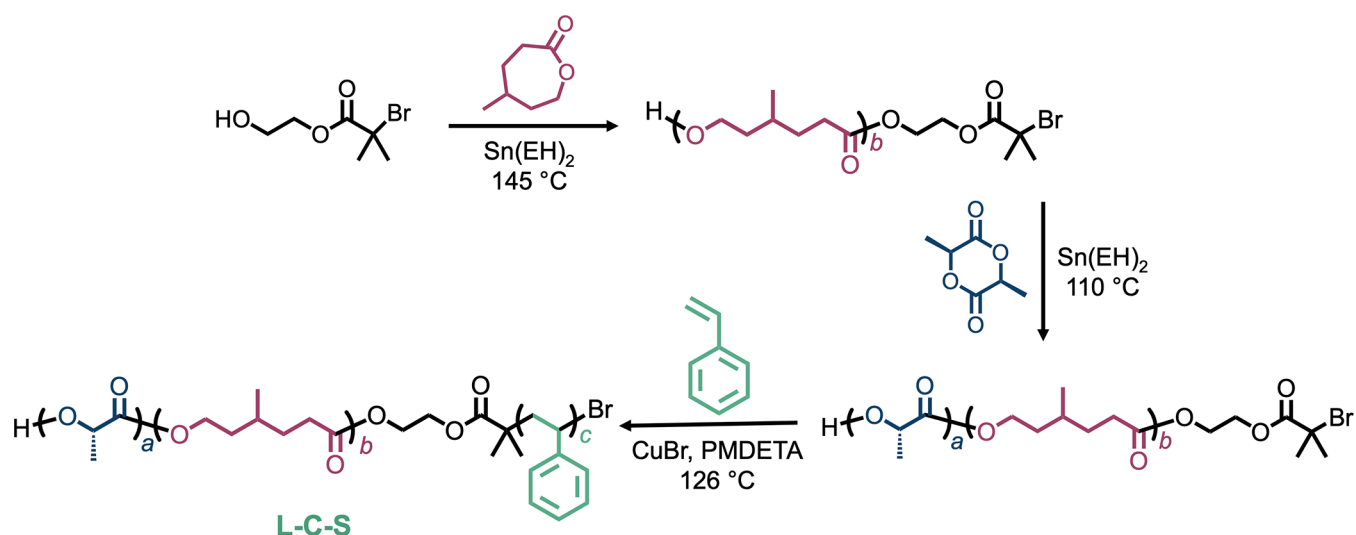


Figure 2. Synthesis of L-C-S triblock terpolymer via sequential ROP and ATRP.

CHARACTERIZATION

An initial comparison of triblocks having 20 vol % hard-block content (L-C-S²⁰, L-C-L²⁰, and S-C-S²⁰) (Figure 3) was

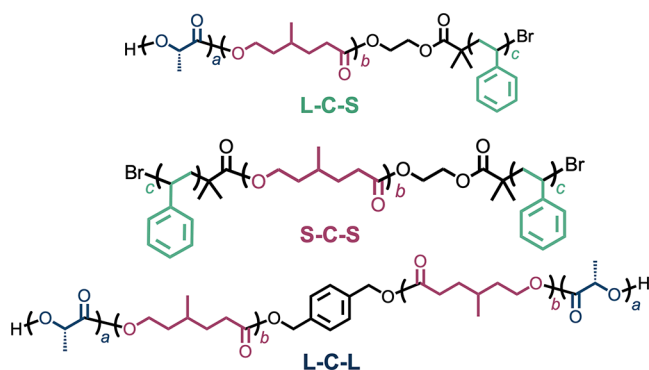


Figure 3. Structures of different triblock thermoplastic elastomers synthesized in this study.

conducted on dogbone specimens that were heat pressed above the melting temperature and immediately quenched (see Supporting Information) to avoid crystalline breakout (Figure S19a,b). Uniaxial stress–strain curves (Figure 4) indicate all three triblocks exhibit comparable strains at break (L-C-S²⁰ = 1700%, L-C-L²⁰ = 1360%, and S-C-S²⁰ = 1650%) due to their similar midblock molecular weights. L-C-S²⁰ yields an ultimate toughness (73 J/cm³) between that of the symmetrical semicrystalline L-C-L²⁰ (138 J/cm³) and amorphous S-C-S²⁰ (54 J/cm³) analogs. Together with the observation that L-C-L²⁰ breaks at the highest stress (28 MPa), these mechanical properties are dominated by the presence or absence of semicrystallinity (Figure S20a,b).^{14,24,30} Interestingly, comparison of the Young's moduli extracted from the stress–strain curve (Table 2) and elastic moduli observed in dynamic mechanical thermal analysis (DMA) (Figure S24) suggest that the L-C-S²⁰ triblock is significantly softer than the corresponding L-C-L²⁰ and S-C-S²⁰ systems. We theorize that the change in chain conformation (i.e., lack of loops) plays a role in reducing the modulus of ABC triblocks due to fewer trapped entanglements per volume within the poly(4-methylcaprolactone) matrix. A lower density of trapped entanglements would

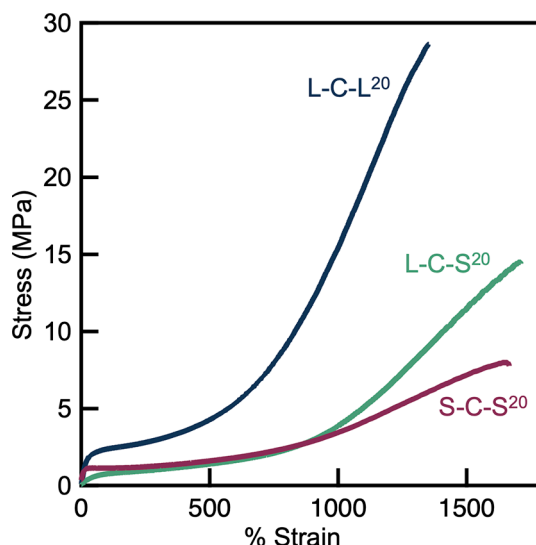


Figure 4. Stress–strain curves in uniaxial extension of ABA (L-C-L, S-C-S) and ABC (L-C-S) triblocks with $f_{\text{Hard}} = 0.20$.

Table 2. Summary of Mechanical Properties for Thermoplastic Elastomers Presented in This Study

TPE ^a	σ_B (MPa) ^b	ϵ_B (%) ^b	U_T (J/cm ³) ^c	E (MPa) ^d
L-C-S ¹⁸	1.8 ± 0.3	1370 ± 40	12 ± 1	0.7 ± 0.2
L-C-S ²⁰	13 ± 2	1700 ± 10	73 ± 11	1.6 ± 0.2
L-C-S ³⁰	19 ± 1	1310 ± 40	101 ± 7	2.6 ± 0.5
L-C-S ⁴⁰	22 ± 1	1180 ± 40	144 ± 10	1.7 ± 0.5
L-C-L ¹⁷	1.8 ± 0.3	1370 ± 40	12 ± 1	0.7 ± 0.2
L-C-L ²⁰	28 ± 1	1360 ± 20	138 ± 2	7 ± 3
L-C-L ²⁹	21 ± 3	1020 ± 90	86 ± 13	23 ± 7
S-C-S ¹⁷	0.4 ± 0.2	190 ± 40	0.8 ± 0.4	2 ± 1
S-C-S ²⁰	8.2 ± 0.6	1650 ± 70	54 ± 8	6 ± 3
S-C-S ³⁰	7.9 ± 0.6	1010 ± 50	39 ± 3	29 ± 17

^aRefers to the triblock chemistry and the total volume fraction of hard block. ^bDetermined from uniaxial tensile testing to the breakpoint of 3 samples extended at 10 mm min⁻¹. ^cCalculated as the area under the stress–strain curve. ^dCalculated from a linear fit at low strains (<10%).

be analogous to a larger midblock entanglement molecular weight, which is known to soften materials.^{24,31}

Following these studies, the elastic recovery of L-C-S triblocks across different volume fractions was compared to both symmetrical L-C-L and S-C-S analogs through cyclic loading experiments to 300% strain at 10 mm min⁻¹ for 10 cycles. Cyclic measurements were conducted in duplicate and allowed to relax for an additional 10 min after removing the applied stress. This additional dwell period was used to compensate for slow relaxation of the glassy polystyrene block (Figure S27a) due to reversible chain pullout from unentangled micellar domains. Significantly, the ABC triblock architecture resulted in superior elastic recovery (98% for L-C-S²⁰) compared to L-C-L²⁰ (95%) and S-C-S²⁰ (90%), highlighting the effect of molecular sequence on the mechanical properties of thermoplastic elastomers (Figure 5).

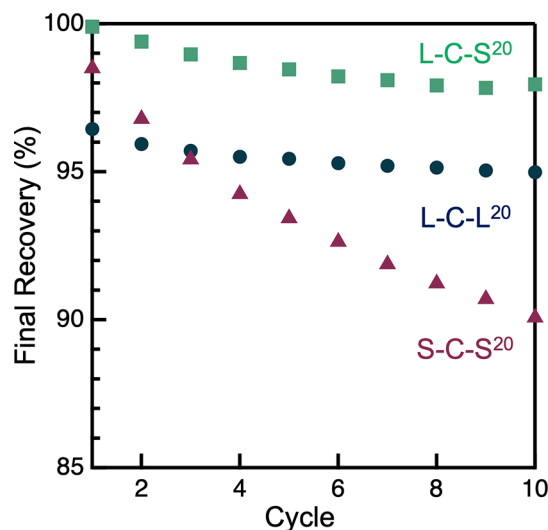


Figure 5. Elastic recovery determined for the $f_{\text{Hard}} = 0.20$ triblock series highlighting the effect of $\sim 100\%$ bridging on strain recovery. The percent recovery is plotted over ten cycles after an initially applied strain of 300%. Final recovery was obtained after removing the applied stress following a dwell period of 10 min as calculated using the final strain after the dwell period (see eq S1).

One of our goals in designing the homologous series of L-C-S, L-C-L, and S-C-S triblocks involved correlating mechanical properties without changing mesostructure. Although small-angle X-ray scattering (SAXS) profiles of L-C-S²⁰ and L-C-L²⁰ appear ordered and consistent with plane group $p2mm$ symmetry (e.g., alternating cylinders),³² the broad and relatively sparse number of peaks prevent a definitive assignment (Figure S22). Furthermore, the S-C-S²⁰ scattering data are featureless due to polystyrene (S) and poly(4-methylcaprolactone) (C) having similar electron densities ($S = 3.3 \times 10^{23}$ electrons cm⁻³, $C = 3.4 \times 10^{23}$ electrons cm⁻³) (Figure S21). To address this characterization challenge, numerical self-consistent field theory (SCFT) simulations were used to investigate phase stability of different candidate morphologies (Figure 6). Building on comprehensive studies from Morse for ABC triblock copolymers,^{26,27} numerical SCFT was used to simulate the phase behavior of ABC systems along the isopleth $f_A = f_C$ using volumetric degrees of polymerization (N_i) and χ_{ij} parameters consistent with the L, C, and S blocks studied herein (see the Supporting Information, Figures S30, S31). Notably, SCFT results support

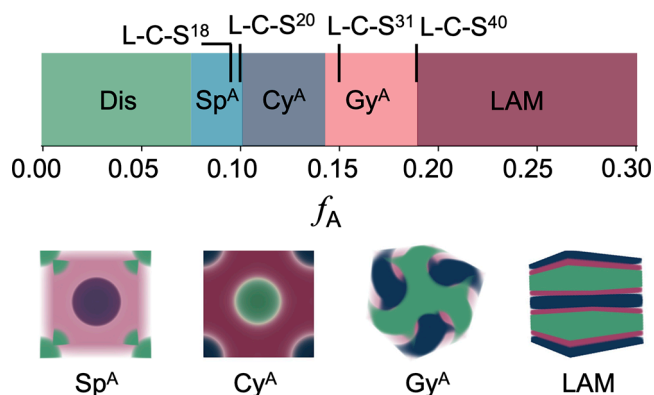


Figure 6. SCFT phase diagram that maps triblock terpolymer phase behavior using the following Flory–Huggins parameters ($\chi_{AC}N = 120.0$, $\chi_{AB}N = 60.0$, and $\chi_{BC}N = 45.8$) (see Supporting Information for additional details) over the isopleth ($f_A = f_C$). Stable phases include disordered (Dis), alternating spheres (Sp^A), alternating cylinders (Cy^A), alternating gyroid (Gy^A), and lamellae (LAM). The tick marks indicate ABC triblock terpolymers synthesized in this study.

the conclusion from mechanical characterization experiments that L-C-S²⁰, L-C-L²⁰, and S-C-S²⁰ form discrete domains of the A and C blocks, e.g., alternating cylinders and sphere morphologies ($f_L = 0.09–0.20$). One important conclusion from the SCFT simulations is a shift in the gyroid–lamellae (Gy–LAM) phase boundary from $f_A \approx 0.32$ in symmetric triblocks to $f_A + f_C \approx 0.36$ for the ABC sequence. In principle, this shift allows for an increased loading of the hard blocks by volume fraction that is reminiscent of more complex architectures.^{16,22,33}

Motivated by these SCFT predictions, L-C-S samples with higher loadings of the L and S hard blocks ($f_{\text{Hard}} = 0.18–0.40$) that would be expected to form discrete spherical or cylindrical domains were synthesized and characterized. As plotted in Figure 7a, ABC triblocks with larger hard-block volume fractions are still extensible (900–1700%) and show strain-hardening behavior typical of semicrystalline thermoplastic elastomers. L-C-S with $f_{\text{Hard}} = 0.40$ reverses this trend with a modest decrease in the strain at break. All of the samples with $f_{L+S} \leq 0.40$ show excellent elastic recovery (Figure 7b) despite SCFT predicting $f_{\text{Hard}} = 0.31$ and 0.40 to fall within the alternating gyroid phase. One possible explanation is that L-C-S³¹ and L-C-S⁴⁰ samples do not exhibit sufficient long-range order as observed in many traditional gyroid phases. Without long-range order, there might not be a truly bi-continuous network that gives rise to the plastic-like mechanical behavior of network phases but instead results in similar mechanical properties to alternating cylinder and sphere samples.³⁴ Another possibility is dispersity or experimental uncertainty in f_A that could cause slight shifts in the expected phase boundary or actual morphology. In contrast, stress–strain data collected on symmetrical triblocks (Figure 8) with volume fractions $f_{\text{Hard}} \geq 0.29$ exhibit irreversible plastic deformation upon straining. This behavior is common for linear symmetrical thermoplastic elastomers where the upper bound of hard-block content is approximately 28%.³⁵ Above this value, the cylinder–gyroid phase transition renders the material plastic, not elastic. As predicted by SCFT and observed experimentally, one way to circumvent this limitation is the use of an ABC sequence with hard A and C blocks, which deflects

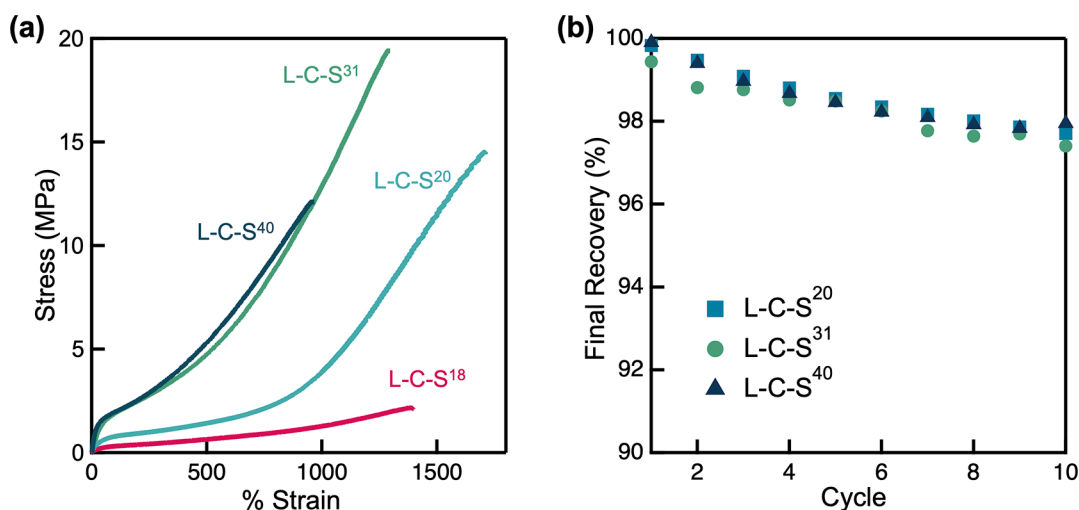


Figure 7. (a) Stress–strain curves for L-C-S over a range of hard-block volume fractions ($f_{\text{Hard}} = 0.18\text{--}0.40$). (b) Elastic recovery for L-C-S samples over ten cycles to 300% strain. Final recovery was measured after removing the applied stress following a dwell period of 10 min.

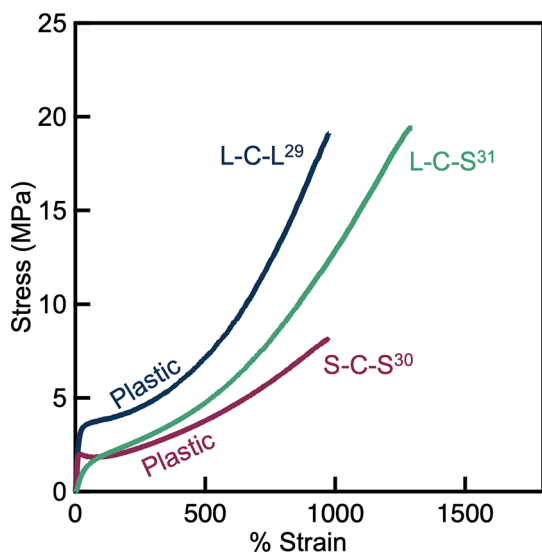


Figure 8. Stress–strain curves in uniaxial extension of ABA (L-C-L, S-C-S) and ABC (L-C-S) triblocks with $f_{\text{Hard}} \approx 0.30$. With increased hard-block content, ABA triblocks exhibit irreversible plastic deformation while ABC triblocks remain elastic.

order–order phase boundaries based on tunable self-assembly parameters.

CONCLUSIONS

Through the development of a robust synthetic strategy to access ABC triblock terpolymers via sequential ring-opening and atom transfer radical polymerization, the importance of molecular architecture on the mechanical performance of block copolymer thermoplastic elastomers was highlighted. The combination of high molecular weight and large χ -parameters enables the design of ABC triblock copolymer sequences that promote full chain bridging of the B block, which enhances elastic recovery compared to symmetrical ABA and CBC analogs. A shift in the of the phase behavior with the ABC sequence also broadens the window of phase stability for discrete cylindrical and spherical morphologies containing larger A/C hard-block content up to $f_{\text{A+C}} \sim 0.40$ while maintaining $>97\%$ elastic recovery. These structural insights

combined with a versatile synthetic platform will motivate future studies into fundamental design principles based on polymer sequence and architecture for next-generation materials with new and improved properties.

ASSOCIATED CONTENT

Supporting Information

The Supporting Information is available free of charge at <https://pubs.acs.org/doi/10.1021/acspolymersau.3c00012>. All curated data are available in the manuscript or the Supporting Information. Raw data are available from a permanent online repository at DOI: 10.25349/D99P6H.

Reagent information, size-exclusion chromatograms and ^1H NMRs of homopolymer, diblocks and triblocks, differential scanning calorimetry of materials, small angle X-ray scattering, wide-angle X-ray scattering, rheological measurements, thermomechanical data, uniaxial tensile testing data, and supplementary SCFT calculations (PDF).

AUTHOR INFORMATION

Corresponding Authors

Christopher M. Bates – Department of Chemistry & Biochemistry, Materials Research Laboratory, Materials Department, and Department of Chemical Engineering, University of California, Santa Barbara, California 93106, United States; orcid.org/0000-0002-1598-794X; Email: cbates@ucsb.edu

Craig J. Hawker – Department of Chemistry & Biochemistry, Materials Research Laboratory, and Materials Department, University of California, Santa Barbara, California 93106, United States; orcid.org/0000-0001-9951-851X; Email: hawker@mrl.ucsb.edu

Authors

Kaitlin R. Albanese – Department of Chemistry & Biochemistry and Materials Research Laboratory, University of California, Santa Barbara, California 93106, United States; orcid.org/0000-0003-1129-8052

Jacob R. Blankenship – Department of Chemistry & Biochemistry and Materials Research Laboratory, University

of California, Santa Barbara, California 93106, United States

Timothy Quah – Department of Chemical Engineering, University of California, Santa Barbara, California 93106, United States

Amy Zhang – Department of Chemical Engineering, University of California, Santa Barbara, California 93106, United States

Kris T. Delaney – Materials Research Laboratory, University of California, Santa Barbara, California 93106, United States; orcid.org/0000-0003-0356-1391

Glenn H. Fredrickson – Materials Research Laboratory, Materials Department, and Department of Chemical Engineering, University of California, Santa Barbara, California 93106, United States; orcid.org/0000-0002-6716-9017

Complete contact information is available at:

<https://pubs.acs.org/10.1021/acspolymersau.3c00012>

Author Contributions

K.R.A., J.R.B., C.M.B., and C.J.H. designed experiments and characterization studies with T.Q., A.Z., K.T.D., and G.H.F. performing SCFT simulations and providing theoretical guidance. K.R.A. and J.R.B. synthesized and characterized materials with all authors contributing to the writing of the manuscript. CRediT: **Kaitlin R Albanese** conceptualization (equal), data curation (equal), writing-original draft (equal), writing-review & editing (equal); **Jacob R Blankenship** data curation (equal), investigation (equal), writing-review & editing (equal); **Timothy Quah** data curation (equal), writing-review & editing (equal); **Amy Zhang** data curation (equal), writing-review & editing (equal); **Kris T. Delaney** data curation (equal), writing-review & editing (equal); **Glenn H. Fredrickson** conceptualization (equal), formal analysis (equal), investigation (equal), writing-original draft (equal), writing-review & editing (equal); **Christopher M. Bates** conceptualization (equal), data curation (equal), formal analysis (equal), funding acquisition (equal), methodology (equal), writing-original draft (equal), writing-review & editing (equal); **Craig J. Hawker** conceptualization (equal), data curation (equal), formal analysis (equal), funding acquisition (equal), project administration (equal), writing-original draft (equal), writing-review & editing (equal).

Notes

The authors declare no competing financial interest.

ACKNOWLEDGMENTS

This research was primarily supported by the US Department of Energy, Office of Basic Energy Sciences, under award number DE-SC0019001. The research reported here made use of shared facilities of the UC Santa Barbara Materials Research Science and Engineering Center (MRSEC, NSF DMR-1720256), a member of the Materials Research Facilities Network (<http://www.mrfn.org>), and the BioPACIFIC Materials Innovation Platform of the National Science Foundation under award no. DMR-1933487. T.Q. acknowledges support from the National Science Foundation Graduate Research Fellowship Program under award number 1650114. Any opinions, findings, and conclusions or recommendations expressed in this material are those of the author(s) and do not necessarily reflect the views of the National Science Foundation. Use was made of computational facilities

purchased with funds from the National Science Foundation (OAC-1925717 and CNS-1725797) and administered by the Center for Scientific Computing (CSC). The CSC is supported by the California NanoSystems Institute and the Materials Research Science and Engineering Center (MRSEC; NSF DMR-1720256) at UC Santa Barbara. The authors would like to thank Dr. Rachel Behrens and Dr. Duyu Chen for helpful discussions.

REFERENCES

- (1) Wang, W.; Lu, W.; Goodwin, A.; Wang, H.; Yin, P.; Kang, N.-G.; Hong, K.; Mays, J. W. Recent Advances in Thermoplastic Elastomers from Living Polymerizations: Macromolecular Architectures and Supramolecular Chemistry. *Prog. Polym. Sci.* **2019**, *95*, 1–31.
- (2) Tallury, S. S.; Mineart, K. P.; Woloszczuk, S.; Williams, D. N.; Thompson, R. B.; Pasquinnelli, M. A.; Banaszak, M.; Spontak, R. J. Communication: Molecular-Level Insights into Asymmetric Triblock Copolymers: Network and Phase Development. *J. Chem. Phys.* **2014**, *141*, 121103.
- (3) Watanabe, H. Slow Dielectric Relaxation of a Styrene-Isoprene-Styrene Triblock Copolymer with Dipole Inversion in the Middle Block: A Challenge to a Loop/Bridge Problem. *Macromolecules* **1995**, *28*, 5006–5011.
- (4) Takano, A.; Kamaya, I.; Takahashi, Y.; Matsushita, Y. Effect of Loop/Bridge Conformation Ratio on Elastic Properties of the Sphere-Forming ABA Triblock Copolymers: Preparation of Samples and Determination of Loop/Bridge Ratio. *Macromolecules* **2005**, *38*, 9718–9723.
- (5) Takahashi, Y.; Hasegawa, S. Shear Effects on the Loop Bridge Ratio of Middle Block Chains in Sphere-Forming ABA Triblock Copolymers Examined by Simple Elongation Measurements. *J. Solid Mech. Mater. Eng.* **2008**, *2*, 473–477.
- (6) Matsen, M. W.; Schick, M. Lamellar Phase of a Symmetric Triblock Copolymer. *Macromolecules* **1994**, *27*, 187–192.
- (7) Matsen, M. W. Equilibrium Behavior of Asymmetric ABA Triblock Copolymer Melts. *J. Chem. Phys.* **2000**, *113*, 5539.
- (8) Matsen, M. W.; Thompson, R. B. Equilibrium Behavior of Symmetric ABA Triblock Copolymer Melts. *J. Chem. Phys.* **1999**, *111*, 7139–7146.
- (9) Drolet, F.; Fredrickson, G. H. Optimizing Chain Bridging in Complex Block Copolymers. *Macromolecules* **2001**, *34*, 5317–5324.
- (10) Shah, M.; Ganesan, V. Chain Bridging in a Model of Semicrystalline Multiblock Copolymers. *J. Chem. Phys.* **2009**, *130*, 054904.
- (11) Rasmussen, K.; Kober, E. M.; Lookman, T.; Saxena, A. Morphology and Bridging Properties of (AB)_n Multiblock Copolymers. *J. Polym. Sci., Part B: Polym. Phys.* **2003**, *41*, 104–111.
- (12) Mori, Y.; Lim, L. S.; Bates, F. S. Consequences of Molecular Bridging in Lamellae-Forming Triblock/Pentablock Copolymer Blends. *Macromolecules* **2003**, *36*, 9879–9888.
- (13) Hamersky, M. W.; Smith, S. D.; Gozen, A. O.; Spontak, R. J. Phase Behavior of Triblock Copolymers Varying in Molecular Asymmetry. *Phys. Rev. Lett.* **2005**, *95*, 168306.
- (14) Burns, A. B.; Register, R. A. Mechanical Properties of Star Block Polymer Thermoplastic Elastomers with Glassy and Crystalline End Blocks. *Macromolecules* **2016**, *49*, 9521–9530.
- (15) Spencer, R. K. W.; Matsen, M. W. Domain Bridging in Thermoplastic Elastomers of Star Block Copolymer. *Macromolecules* **2017**, *50*, 1681–1687.
- (16) Blankenship, J. R.; Levi, A. E.; Goldfeld, D. J.; Self, J. L.; Alizadeh, N.; Chen, D.; Fredrickson, G. H.; Bates, C. M. Asymmetric Miktoarm Star Polymers as Polyester Thermoplastic Elastomers. *Macromolecules* **2022**, *55*, 4929–4936.
- (17) Deacy, A. C.; Gregory, G. L.; Sulley, G. S.; Chen, T. T. D.; Williams, C. K. Sequence Control from Mixtures: Switchable Polymerization Catalysis and Future Materials Applications. *J. Am. Chem. Soc.* **2021**, *143*, 10021–10040.

- (18) Schmalz, H.; Böker, A.; Lange, R.; Krausch, G.; Abetz, V. Synthesis and Properties of ABA and ABC Triblock Copolymers with Glassy (A), Elastomeric (B), and Crystalline (C) Blocks. *Macromolecules* **2001**, *34*, 8720–8729.
- (19) Brinkmann-Rengel, S.; Abetz, V.; Stadler, R.; Thomas, E. L. Thermoplastic Elastomers Based on ABA-and ABC-Triblock Copolymers. *Kautsch. Gummi Kunstst.* **1999**, *52*, 806–813.
- (20) Fetters, L. J.; Morton, M. Synthesis and Properties of Block Polymers. I. Poly- α -Methylstyrene-Polyisoprene-Poly- α -Methylstyrene. *Macromolecules* **1969**, *2*, 453–458.
- (21) Bolton, J. M.; Hillmyer, M. A.; Hoyer, T. R. Sustainable Thermoplastic Elastomers from Terpene-Derived Monomers. *ACS Macro Lett.* **2014**, *3*, 717–720.
- (22) Lequeieu, J.; Koeper, T.; Delaney, K. T.; Fredrickson, G. H. Extreme Deflection of Phase Boundaries and Chain Bridging in A(BA')_n Miktoarm Star Polymers. *Macromolecules* **2020**, *53*, 513–522.
- (23) Liffland, S.; Hillmyer, M. A. Enhanced Mechanical Properties of Aliphatic Polyester Thermoplastic Elastomers through Star Block Architectures. *Macromolecules* **2021**, *54*, 9327–9340.
- (24) Watts, A.; Kurokawa, N.; Hillmyer, M. A. Strong, Resilient, and Sustainable Aliphatic Polyester Thermoplastic Elastomers. *Biomacromolecules* **2017**, *18*, 1845–1854.
- (25) Bailey, T. S. Morphological Behavior Spanning the Symmetric AB and ABC Block Copolymer States; University of Minnesota, 2001.
- (26) Qin, J.; Bates, F. S.; Morse, D. C. Phase Behavior of Nonfrustrated ABC Triblock Copolymers: Weak and Intermediate Segregation. *Macromolecules* **2010**, *43*, 5128–5136.
- (27) Tyler, C. A.; Qin, J.; Bates, F. S.; Morse, D. C. SCFT Study of Nonfrustrated ABC Triblock Copolymer Melts. *Macromolecules* **2007**, *40*, 4654–4668.
- (28) Zalusky, A. S.; Olayo-Valles, R.; Wolf, J. H.; Hillmyer, M. A. Ordered Nanoporous Polymers from Polystyrene–Polylactide Block Copolymers. *J. Am. Chem. Soc.* **2002**, *124*, 12761–12773.
- (29) Höcker, H.; Shih, H.; Flory, P. J. Thermodynamics of Polystyrene Solutions. Part 3.—Polystyrene and Cyclohexane. *Trans. Faraday Soc.* **1971**, *67*, 2275–2281.
- (30) Panthani, T. R.; Bates, F. S. Crystallization and Mechanical Properties of Poly(*l*-Lactide)-Based Rubbery/Semicrystalline Multi-block Copolymers. *Macromolecules* **2015**, *48*, 4529–4540.
- (31) Holden, G.; Bishop, E. T.; Legge, N. R. Thermoplastic Elastomers. *J. Polym. Sci., Part C: Polym. Symp.* **1969**, *26*, 37–57 Wiley Online Library.
- (32) Brinkmann, S.; Stadler, R.; Thomas, E. L. New Structural Motif in Hexagonally Ordered Cylindrical Ternary (ABC) Block Copolymer Microdomains. *Macromolecules* **1998**, *31*, 6566–6572.
- (33) Lynd, N. A.; Oyerokun, F. T.; O'Donoghue, D. L.; Handlin, D. L.; Fredrickson, G. H. Design of Soft and Strong Thermoplastic Elastomers Based on Nonlinear Block Copolymer Architectures Using Self-Consistent-Field Theory. *Macromolecules* **2010**, *43*, 3479–3486.
- (34) Wang, C.-Y.; Lodge, T. P. Kinetics and Mechanisms for the Cylinder-to-Gyroid Transition in a Block Copolymer Solution. *Macromolecules* **2002**, *35*, 6997–7006.
- (35) Matsen, M. W. Effect of Architecture on the Phase Behavior of AB-Type Block Copolymer Melts. *Macromolecules* **2012**, *45*, 2161–2165.